First published February 10, 2010; doi:10.1152/ajpregu.00336.2009.

Urinary tract obstruction induces transient accumulation of COX-2-derived prostanoids in kidney tissue

Rikke Nørregaard,[1,2] Boye L Jensen,[4] Sukru Oguzkan Topcu,[1,2] Guixian Wang,[1,2] Horst Schweer,[6] Søren Nielsen,[1,3] and Jørgen Frøkiær[1,2,5]

[1]The Water and Salt Research Center, [2]Institute of Clinical Medicine and [3]Institute of Anatomy, University of Aarhus, Aarhus; [4]Department of Physiology and Pharmacology, University of Southern Denmark, Odense; [5]Department of Clinical Physiology and Nuclear Medicine, Aarhus University Hospital-Skejby, Aarhus, Denmark; and [6]Department of Pediatrics, Philipps University Marburg, Marburg, Germany

Submitted 15 June 2009; accepted in final form 8 February 2010

Nørregaard R, Jensen BL, Topcu SO, Wang G, Schweer H, Nielsen S, Frøkiær J. Urinary tract obstruction induces transient accumulation of COX-2-derived prostanoids in kidney tissue. *Am J Physiol Regul Integr Comp Physiol* 298: R1017–R1025, 2010. First published February 10, 2010; doi:10.1152/ajpregu.00336.2009.—Inhibitors of cyclooxygenase (COX)-2 prevent suppression of aquaporin-2 and reduce polyuria in the acute phase after release of bilateral ureteral obstruction (BUO). We hypothesized that BUO leads to COX-2-mediated local accumulation of prostanoids in inner medulla (IM) tissue. To test this, rats were subjected to BUO and treated with selective COX-1 or COX-2 inhibitors. Tissue was examined at 2, 6, 12, and 24 h after BUO. COX-2 protein abundance increased in IM 12 and 24 h after onset of BUO but did not change in cortex. COX-1 did not change at any time points in any region. A full profile of all five primary prostanoids was obtained by mass spectrometric determination of PGE_2, $PGF_{2\alpha}$, 6-keto-$PGF_{1\alpha}$, PGD_2, and thromboxane (Tx) B_2 concentrations in kidney cortex/outer medulla and IM fractions. IM concentration of PGE_2, 6-keto-$PGF_{1\alpha}$, and $PGF_{2\alpha}$ was increased at 6 h BUO, and PGE_2 and $PGF_{2\alpha}$ increased further at 12 h BUO. TxB_2 increased after 12 h BUO. 6-keto-$PGF_{1\alpha}$ remained significantly increased after 24 h BUO. The COX-2 inhibitor parecoxib lowered IM PGE_2, TxB_2, 6-keto-$PGF_{1\alpha}$, and $PGF_{2\alpha}$ below vehicle-treated BUO and sham rats at 6, 12 and, 24 h BUO. The COX-1 inhibitor SC-560 lowered PGE_2, $PGF_{2\alpha}$, and PGD_2 in IM compared with untreated 12 h BUO, but levels remained significantly above sham. In cortex tissue, PGE_2 and 6-keto-$PGF_{1\alpha}$ concentrations were elevated at 6 h only. In conclusion, COX-2 activity contributes to the transient increase in prostacyclin metabolite 6-keto-$PGF_{1\alpha}$ and TxB_2 concentration in the kidney IM, and COX-2 is the predominant isoform that is responsible for accumulation of PGE_2 and $PGF_{2\alpha}$ with minor, but significant, contributions from COX-1. PGD_2 synthesis is mediated exclusively by COX-1. In BUO, therapeutic interventions aimed at the COX-prostanoid pathway should target primarily COX-2.

bilateral ureteral obstruction; cyclooxygenase-2; mass spectrometric

CLINICALLY, URINARY TRACT obstruction accounts for a major proportion of renal insufficiency (14). Complete urinary tract obstruction is associated with major changes in glomerular filtration rate (GFR), renal blood flow (RBF), and tubular functions. GFR declines immediately after onset of obstruction, whereas RBF slowly is reduced with progressive increase in pelvic pressure (4, 17). In parallel, the tubular reabsorption of sodium and water is altered (15). The decrease in GFR and RBF is partly mediated by the vasoconstrictors ANG II and thromboxane A_2 (TxA_2) (5, 6, 30). Vasodilatory prostaglandins such as prostaglandin E_2 (PGE_2) and I_2 (PGI_2) may be compensatorily released to prevent decrease in GFR and RBF by antagonizing these vasoconstrictor agents (4). PGE_2 and PGI_2 are not only vasodilators, but do also have natriuretic and diuretic properties (23, 24).

Previous studies indicate that cyclooxygenase (COX) activity contributes to renal function changes immediately after onset of ureteral obstruction (2, 19, 20). We, and others, have demonstrated that expression of COX-2 mRNA and protein, but not COX-1, is markedly increased in the inner medulla (IM) in response to unilateral ureteral obstruction (UUO) (3) and bilateral ureteral obstruction (BUO) (2, 19). Administration of a selective COX-2 inhibitor prevents downregulation of aquaporin-2 (AQP2) in inner medullary collecting ducts (19) and attenuates the polyuria observed typically during the first day after release of 24 h BUO. Urinary excretion of the PGE_2 and PGI_2 metabolite 6-keto-$PGF_{1\alpha}$ increased significantly after release of BUO compared with sham operation, and this increase was abolished by administration of a COX-2 inhibitor, parecoxib (20). These findings demonstrate that COX-2 expression is induced after obstruction and that the resulting PGE_2 generation may explain the changes in kidney function.

During experimental ureteral obstruction, it is not possible to measure prostanoid excretion, and, after release of ureteral obstruction, the prostanoids detected in urine likely represent a product arising from glomerular filtration, tubular secretion, and release from infiltrating inflammatory cells and from the epithelium lining the urinary tract wall and does not exclusively represent renal medullary COX-2 activity. We hypothesized that the marked increase in renal medullary interstitial cell COX-2 expression after ureteral obstruction causes a significant increase in, particularly, PGE_2 synthesis and tissue concentration in the renal medulla. PGE_2 is known to inhibit vasopressin-stimulated osmotic water permeability and sodium transport in collecting duct principal cells (10, 23).

To address the hypotheses, a kinetic study was designed to allow for precise determination of temporal correlations between COX-1 and COX-2 expression and tissue prostanoid concentration after ureteral obstruction for 2, 6, 12, and 24 h. A full prostanoid profile [PGE_2, $PGF_{2\alpha}$, PGI_2 (6-keto-$PGF_{1\alpha}$), and TxA_2 (TxB_2)] was determined in extracts of IM and cortical/outer medulla (C/OM) tissue fractions by gas chromatography/tandem mass spectrometry. To define the contribution of distinct COX activities to the tissue prostanoid profile after BUO, the COX-1-selective blocker SC-560 and COX-2-

Address for reprint requests and other correspondence: J. Frøkiær, The Water and Salt Research Center, Institute of Clinical Medicine, Univ. of Aarhus, Dept. of Clinical Physiology and Nuclear Medicine, Aarhus Univ. Hospital-Skejby, Brendstrupgaardsvej, DK-8200 Aarhus N, Denmark (e-mail: JF@KI.AU.DK).

selective blocker parecoxib were administrated in separate experimental series before and during ureteral obstruction and compared with vehicle-treated BUO rats. Subsequently, kidneys were harvested and dissected in C/OM and IM fractions that were analyzed for prostanoid tissue profile.

METHODS

Experimental Animals

All procedures conformed with the Danish national guidelines for the care and handling of animals and to the published guidelines from the National Institutes of Health. The animal protocols were approved by the board of the Institute of Clinical Medicine, University of Aarhus, according to the licenses for use of experimental animals issued by the Danish Ministery of Justice. Studies were performed in male Munich-Wistar rats initially weighing 220 g (Møllegaard Breeding Centre, Eiby, Denmark). The rats had free access to a standard rodent diet (Altromin, Lage, Germany) and tap water. During the experiments, rats were kept in individual metabolic cages, with a 12:12-h light-dark cycle, a temperature of 21 ± 2°C, and a humidity of 55 ± 2%. Rats were allowed to acclimatize to the cages 3–4 days before surgery. The rats were placed on anesthesia with isoflurane (Abbott Scandinavia), and, during the operation, the rats were placed on a heating pad to maintain rectal temperature at 37–38°C. Through a midline abdominal incision, both ureters were exposed and then occluded with a 5–0 silk ligature.

Rats were allocated to the protocols indicated below. Age- and time-matched, sham-operated controls were prepared and were observed in parallel with each BUO group.

For experiments with a selective COX-2 inhibitor, the protocols were as follows.

Protocol 1. BUO was induced for 2, 6, 12, and 24 h ($n = 6$ for each time point). The left kidney was prepared for semiquantitative immunoblotting and the right for measurements of prostanoids. In another group, the left kidney was prepared for immunohistochemistry.

Protocol 2. Sham-operated controls were prepared in parallel ($n = 6$ for each time point). The left kidney was prepared for semiquantitative immunoblotting and the right for measurements of prostanoids. In another group, the left kidney was prepared for immunohistochemistry.

Protocol 3. BUO was induced for 2, 6, 12, and 24 h, and osmotic minipumps (Alzet, Scanbur, Denmark) with the selective COX-2 inhibitor parecoxib (Pfizer, Ballerup, Denmark) dissolved in saline (40 mg/ml) were surgically implanted subcutaneously 24 h before ureteral obstruction and given at a rate of 5 $mg \cdot kg^{-1} \cdot day^{-1}$ during the time of obstruction ($n = 6$ for each time point). Administration of 5 $mg \cdot kg^{-1} \cdot day^{-1}$ parecoxib was chosen according to the pharmacological profile of parecoxib as previously demonstrated (21). In this group, the left kidney was prepared for semiquantitative immunoblotting and the right kidney for measurements of prostanoids.

For experiments with a selective COX-1 inhibitor, the protocols were as follows.

Rats were deprived of food but had free access to water for 12 h before administration of vehicle or inhibitors. The compound was administrated orally, via gavage needle in polyethylene glycol 600 vehicle (10 mg/kg), for a period of 2 h before the obstruction was performed and during the obstructed period. The doses were selected based on the published pharmacological profile of SC-560 (27).

Protocol 4. BUO was induced for 12 and 24 h ($n = 6$ for each time point), and rats were treated with vehicle. The right kidney was prepared for measurements of prostanoids.

Protocol 5. Sham-operated controls were prepared in parallel and treated with vehicle ($n = 6$ for each time point). The right kidney was prepared for measurements of prostanoids.

Protocol 6. BUO was induced for 12 and 24 h, and rats were treated with the selective COX-1 inhibitor SC-560 (Cayman Chemicals, Ann Arbor, MI) ($n = 7$ for each time point). The right kidney was prepared for measurements of prostanoids.

Measurement of Prostanoid Concentration in Kidney Tissue

The tissue was homogenized in ice-cold PBS buffer containing 10 μmol/l indomethacin. Protein concentration was measured using the Pierce BCA protein assay kit. In an isotope dilution assay, PGE_2, the PGI_2 metabolite 6-keto-$PGF_{1\alpha}$, $PGF_{2\alpha}$, PGD_2 and TxB_2 were determined in IM and C/OM using gas chromatography/tandem mass spectrometry (GC-MS-MS). After addition of deuterated internal standards, the prostanoids were derivatized to methoximes and extracted with ethyl acetate-hexane. The samples were further derivatized to the pentafluorobenzyl esters and purified using thin-layer chromatography (TLC). Three zones were scraped from the TLC. The prostanoid derivatives were converted to the trimethylsilyl ethers and the products quantified using GC-MS-MS.

GC-MS-MS Analysis

A Finnigan MAT TSQ700 GC-MS-MS equipped with a Varian 3400 gas chromatograph and a CTC A200S autosampler was used. Gas chromatography of prostanoid derivatives was carried out on a (J & W) DB-1 (20 m, 0.25 mm ID, 0.25-μm film thickness) capillary column (Analyt, Mühlheim, Germany) in the splitless mode. GC-MS-MS parameters were exactly as described by Schweer et al. (26).

Tissue Handling for Immunoblotting

The tissue (C/OM and IM) was homogenized in dissecting buffer [0.3 M sucrose, 25 mM imidazole, 1 mM EDTA, pH 7.2, containing the following protease inhibitors: 8.5 μM leupeptin (serine and cysteine protease inhibitor; Sigma-Aldrich) and 0.4 mM pefabloc (serineprotease inhibitor; Roche)]. Moreover, the dissecting buffer for IM was added following phosphatase inhibitors sodium ortho-Vanadat (Sigma-Aldrich), Na-F (Merck), and okadic acid (Calbiocham). The tissue was homogenized for 30 s at 1,250 rpm by an Ultra-Turrax T8 homogenizer (IKA Labortechnik) and then centrifuged at 1,500 *g* at 4°C for 15 min. Gel samples were prepared from the supernatant in Laemmli sample buffer containing 2% SDS. The total protein concentration of the homogenate was measured using a Pierce BCA protein assay kit (Roche).

Electrophoresis and Immunoblotting

Homogenized samples from C/OM and IM were run on 12% polyacrylamide minigels (Bio-Rad Mini Protean II). For each gel, an identical gel was run in parallel and subjected to Coomassie staining. The Coomassie-stained gel was applied to determine identical loading or to allow for correction for minor variations in loading.

Samples were run on 9, 10, and 12% polyacrylamide gels (Protean II; Bio-Rad). Proteins were transferred to a nitrocellulose membrane (Hybond ECL RPN 3032D; Amersham Pharmacia Biotech). Afterward, the blots were blocked with 5% nonfat dry milk in PBS-T (80 mM Na_2HPO_4, 20 mM NaH_2PO_4, 100 mM NaCl, 0.1% Tween 20, adjusted to pH 7.4). After being washed in PBS-T, the blots were incubated with primary antibodies overnight at 4°C. Antigen-antibody complex was visualized with horseradish peroxidase-conjugated secondary antibodies (P448, diluted 1:3,000; DAKO, Glostrup, Denmark) using the enhanced chemiluminiscence system (ECL; Amersham Pharmacia Biotech). Immunolabeling controls were performed using peptide-absorbed antibody.

Primary Antibodies

For semiquantitative immunoblotting and immunohistochemistry, we used previously characterized monoclonal and polyclonal antibodies summarized as follows: COX-1 (catalog no. 160109; Cayman Chemical, Ann Arbor, MI), an affinity-purified rabbit polyclonal antibody against COX-1; COX-2 (catalog no. 160126; Cayman

Chemical), an affinity-purified rabbit polyclonal antibody against COX-2; PGE_2 synthase (PGES; catalog no. 160140; Cayman Chemical), an affinity-purified rabbit polyclonal antibody against PGES; AQP2 (H7661), an affinity-purified antibody to AQP2, as previously described (18).

Immunohistochemistry

The kidneys from BUO rats and sham-operated control rats were fixed by retrograde perfusion via the abdominal aorta with 3% paraformaldehyde in 0.1 M cacodylate buffer, pH 7.4. Moreover, the kidneys were immersion fixed for 1 h and washed 3 × 10 min with 0.1 M cacodylate buffer. The kidney blocks were dehydrated and embedded in paraffin. The paraffin-embedded tissues were cut in 2-μm sections on a rotary microtome (Leica Microsystems, Herlev, Denmark).

For immunoperoxidase labeling, the sections were deparaffinized and rehydrated. Endogenous peroxidase activity was blocked with 5% H_2O_2 in absolute methanol for 10 min at room temperature. To expose antigens, kidney sections were boiled in a target retrieval solution (1 mmol/l Tris, pH 9.0, with 0.5 mM EGTA) for 10 min. After cooling, nonspecific binding was prevented by incubating the sections in 50 mM NH_4Cl in PBS for 30 min, followed by blocking in PBS containing 1% BSA, 0.05% saponin, and 0.2% gelatine. Sections were incubated with primary antibodies diluted in PBS with 0.1% BSA and 0.3% Triton X-100 overnight at 4°C. After being washed 3 × 10 min with PBS supplemented with 0.1% BSA, 0.05% saponin, and 0.2% gelatine, the sections were incubated with horseradish peroxidase-conjugated secondary antibody (P448, goat anti-rabbit immunoglobulin; DAKO) for 1 h at room temperature. After being rinsed with PBS wash buffer, the sites of antibody-antigen reactions were visualized with 0.05% 3,3′-diaminobenzidine tetrachloride (Kem-en Tek, Copenhagen, Denmark) dissolved in distilled water with 0.1% H_2O_2. The light microscope was carried out with Lecia DMRE (Leica Microsystem, Herlev, Denmark).

Statistics

Values are presented as means ± SE. Statistical comparisons between experimental groups were made by a standard unpaired *t*-test. *P* values <0.05 were considered significant.

RESULTS

Time Course of Changes in Total Prostanoid Tissue Concentration in Renal IM and C/OM in Response to BUO

To evaluate the relative importance of each COX isoform for intrarenal prostanoid synthesis in response to ureteral obstruction, rats were subjected either to sham operation or BUO for 2, 6, 12, and 24 h. BUO rats were subcutaneously given either vehicle or a selective COX-2 inhibitor, parecoxib (5 $mg \cdot kg^{-1} \cdot day^{-1}$), through osmotic minipumps, and tissue prostanoid concentration was determined in IM and C/OM tissue fractions by GC-MS-MS (Fig. 1). Tissue concentration was significantly higher in the IM compared with the C/OM fraction for each measured prostanoid at all time points (~10–150 times; Fig. 1). In IM tissue, the ratios between concentration of prostanoid groups in sham rats were $PGE_2 > TxB_2 > PGF_{2\alpha} >$ 6-keto-$PGF_{1\alpha} > PGD_2$, whereas in C/OM there were no significant differences in concentration (Fig. 1). The prostacyclin metabolite 6-keto-$PGF_{1\alpha}$ and $PGF_{2\alpha}$ tissue concentrations displayed the earliest detectable change at the tissue level. Tissue concentrations of PGE_2, the PGI_2 metabolite 6-keto-$PGF_{1\alpha}$, and $PGF_{2\alpha}$ increased significantly at 6 h after BUO in IM compared with sham (Table 1). After 12 h, the IM concentrations of

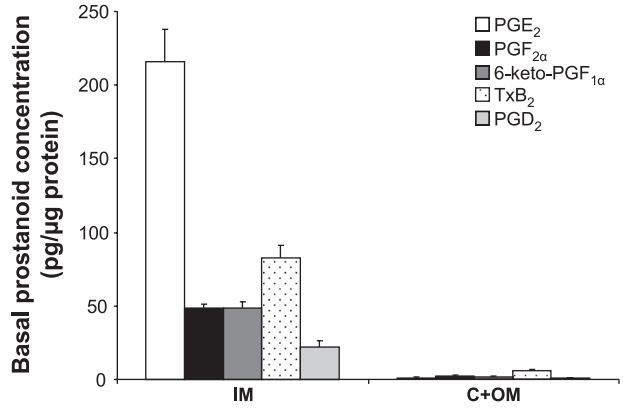

Fig. 1. Basal prostanoid profiles in renal inner medulla (IM) and cortex + outer medulla (C + OM). Bars in each group from left to right represent PGE_2, $PGF_{2\alpha}$, 6-keto-$PGF_{1\alpha}$, thromboxane (Tx) B_2, and PGD_2; $n = 6$ rats in each group.

PGE_2, $PGF_{2\alpha}$, and TxB_2 were all significantly elevated in BUO rats compared with sham (Table 1). At 24 h BUO, 6-keto-$PGF_{1\alpha}$ IM concentration remained significantly elevated, whereas $PGF_{2\alpha}$, PGE_2, and TxB_2 returned to levels not significantly different from levels in sham-operated control rats (Table 1). PGD_2 tissue concentration was not altered in IM by BUO compared with sham (Table 1).

In the kidney C/OM tissue fraction, PGE_2 and 6-keto-$PGF_{1\alpha}$ concentrations increased significantly at 6 h post-BUO compared with sham-operated rats. Furthermore, TxB_2 concentration in C/OM was increased in response to 24 h BUO (Table 2).

Effect of a Selective COX-2 Inhibitor on Kidney Tissue Prostanoid Concentration in Response to BUO

COX-2 inhibition with parecoxib (5 $mg \cdot kg^{-1} \cdot day^{-1}$) suppressed PGE_2 tissue concentration compared with BUO vehicle at 6, 12, and 24 h in IM. After BUO for 6, 12, and 24 h, parecoxib treatment suppressed PGE_2 levels significantly below that observed in sham-operated and vehicle-treated BUO rats (Table 1). Parecoxib attenuated both prostacyclin metabolite 6-keto-$PGF_{1\alpha}$ and $PGF_{2\alpha}$ concentration in IM compared with BUO and sham operation at all time points (2, 6, 12, and 24 h; Table 1). Moreover, parecoxib lowered the IM tissue concentration of the TxA_2 metabolite TxB_2 significantly at 6, 12, and 24 h compared with vehicle-infused BUO rats and sham-operated rats (Table 1). In marked contrast, IM tissue concentration of PGD_2 was significantly elevated after 2 and 6 h in BUO rats treated with parecoxib compared with vehicle-treated BUO rats, whereas, at 12 h BUO, the PGD_2 concentration was lower than in BUO vehicle rats. At 24 h, there were no differences in PGD_2 concentrations (Table 1).

In C/OM, administration of parecoxib did not significantly change the BUO-induced increase in PGE_2 and 6-keto-$PGF_{1\alpha}$ at 6 h BUO. However, at 24 h BUO, 6-keto-$PGF_{1\alpha}$ tissue concentration was significantly suppressed by administration of parecoxib compared with vehicle-treated BUO rats (Table 2). Parecoxib administration suppressed the concentration of TxB_2 at 12 and 24 h BUO compared with BUO vehicle and sham-operated rats (Table 2). $PGF_{2\alpha}$ in C/OM tissue was lowered significantly by parecoxib compared with BUO and sham rats after 24 h (Table 2). Similar to IM, PGD_2 concentration in C/OM tissue responded differently compared with

Table 1. *Profile of prostanoid production in inner medulla in nontreated and parecoxib-treated BUO rats for 2, 6, 12, and 24 h and sham-operated control rats*

Time, h	PGE_2	6-Keto-$PGF_{1\alpha}$	$PGF_{2\alpha}$	TxB_2	PGD_2
2					
Sham	140 ± 12.5	24 ± 1.6	31 ± 3.0	40 ± 4.7	15 ± 2.0
BUO	144 ± 26.7	27 ± 2.1	27 ± 5.1	26 ± 5.6	10 ± 1.9
BUO + pc	102 ± 3.8	13 ± 1.9†‡	15 ± 0.5†‡	31 ± 3.2	27 ± 1.6†‡
6					
Sham	136 ± 11.0	20 ± 1.0	33 ± 3.0	52 ± 6.8	18 ± 2.5
BUO	188 ± 14.4*	29 ± 2.8*	53 ± 4.3*	62 ± 4.9	19 ± 2.1
BUO + pc	93 ± 9.8†‡	10 ± 1.2†‡	21 ± 1.2†‡	27 ± 2.0†‡	34 ± 9.8†‡
12					
Sham	125 ± 4.8	35 ± 8.9	50 ± 13.3	82 ± 24.6	39 ± 12.8
BUO	319 ± 57.2*	48 ± 4.2	102 ± 11.1*	164 ± 17.2*	62 ± 9.2
BUO + pc	64 ± 6.8†‡	17 ± 2.5†‡	20 ± 2.4†‡	38 ± 3.0†‡	26 ± 4.3†
24					
Sham	215 ± 22.4	52 ± 4.7	48 ± 2.8	89 ± 9.9	22 ± 4.3
BUO	174 ± 24.3	76 ± 10.7*	54 ± 9.0	108 ± 16.8	19 ± 2.3
BUO + pc	46 ± 2.4†‡	12 ± 1.5†‡	14 ± 1.0†‡	32 ± 4.0†‡	14 ± 1.2

Values are means ± SE for $n = 6$ rats in each group. Units are pg/μg tissue. TxB_2, thromboxane B_2; BUO, bilateral ureteral obstruction; pc, parecoxib. $P < 0.05$, respective prostanoids in nontreated BUO vs. sham-operated control rats (*), respective prostanoids in nontreated BUO vs. parecoxib-treated BUO rats (†), and respective prostanoids in parecoxib-treated BUO vs. sham-operated control rats (‡).

the other prostanoids; tissue concentration was elevated significantly by parecoxib at 6, 12, and 24 h compared with BUO vehicle and sham-operated rats (Table 2).

Effect of a Selective COX-1 Inhibitor on Kidney Tissue Prostanoid Concentration in Response to BUO

To investigate the contribution of COX-1 activity to the BUO-induced changes in prostanoid production in the IM, a separate series of rats were subjected to 12 and 24 h BUO and treated with the selective COX-1 inhibitor SC-560 (10 mg/kg) or vehicle. The absolute level of tissue prostanoid concentrations was lower in this series, but the relative changes in response to BUO were similar to the previous series. Thus, all five measured prostanoids exhibited an elevated tissue concentration after 12 h BUO, and, after 24 h, PGE_2 and 6-keto-$PGF_{1\alpha}$ remained significantly elevated. Administration of SC-560 resulted in a significant lower tissue concentration of PGE_2, $PGF_{2\alpha}$, and PGD_2 at 12 h compared with vehicle-treated BUO rats. Although significantly suppressed compared with BUO vehicle rats at 12 h, PGE_2 and $PGF_{2\alpha}$ tissue concentrations were still significantly elevated above sham, whereas PGD_2 was essentially normalized by COX-1 inhibition (Table 3).

Time Course of Changes in COX Protein Abundance and Localization in Response to BUO

The abundance of COX-1 protein did not change in response to BUO in IM and C/OM during the time course of the experiment (Fig. 2, *A* and *B*). COX-2 protein abundance increased significantly in IM tissue after 12 and 24 h of BUO (Fig. 3*A*). COX-2 protein abundance did not change significantly in the C/OM tissue fraction during the experiment (Fig. 3*B*). Immunohistochemical staining of kidney IM sections for COX-2 confirmed essentially the Western blotting results: at the base of IM in rats subjected to 12 and 24 h of BUO (Fig. 4, *F* and *H*),

Table 2. *Profile of prostanoid production in cortex/outer medulla in nontreated and parecoxib-treated BUO rats for 2, 6, 12, and 24 h and sham-operated control rats*

Time, h	PGE_2	6-Keto-$PGF_{1\alpha}$	$PGF_{2\alpha}$	TxB_2	PGD_2
2					
Sham	1.5 ± 0.17	2.0 ± 0.42	1.9 ± 0.32	4.3 ± 0.24	0.62 ± 0.10
BUO	1.5 ± 0.24	1.8 ± 0.35	2.0 ± 0.29	4.9 ± 0.80	0.51 ± 0.08
BUO + pc	1.1 ± 0.21	1.3 ± 0.16	1.8 ± 0.50	3.8 ± 0.46	0.83 ± 0.25
6					
Sham	0.8 ± 0.03	1.1 ± 0.13	1.0 ± 0.07	2.8 ± 0.04	0.32 ± 0.03
BUO	1.7 ± 0.18*	2.5 ± 0.20*	1.4 ± 0.10	2.9 ± 0.15	0.33 ± 0.03
BUO + pc	1.3 ± 0.07	1.6 ± 0.20	1.5 ± 0.25	2.7 ± 0.45	0.97 ± 0.12†‡
12					
Sham	1.2 ± 0.11	1.5 ± 0.28	1.0 ± 0.20	3.0 ± 0.33	0.28 ± 0.04
BUO	1.5 ± 0.16	1.7 ± 0.16	1.4 ± 0.20	3.4 ± 0.56	0.41 ± 0.11
BUO + pc	1.8 ± 0.24	1.0 ± 0.09	1.0 ± 0.09	1.8 ± 0.08†‡	0.76 ± 0.06†‡
24					
Sham	1.0 ± 0.10	1.8 ± 0.28	2.4 ± 0.26	4.6 ± 0.68	0.52 ± 0.10
BUO	1.8 ± 0.40	3.2 ± 0.76	1.9 ± 0.35	7.3 ± 1.08*	0.50 ± 0.10
BUO + pc	1.5 ± 0.14	1.4 ± 0.17†	1.0 ± 0.10†‡	2.1 ± 0.38†‡	0.83 ± 0.06†‡

Values are means ± SE for $n = 6$ rats in each group. Units are pg/μg tissue. $P < 0.05$, respective prostanoids in nontreated BUO vs. sham-operated control rats (*), respective prostanoids in nontreated BUO vs. parecoxib-treated BUO rats (†), and respective prostanoids in parecoxib-treated BUO vs. sham-operated control rats (‡).

Table 3. *Profile of prostanoid production in inner medulla of vehicle-treated rats and rats treated with a cyclooxygenase-1 inhibitor (SC-560) in BUO rats for 12 and 24 h and sham-operated control rats*

Time, h	PGE_2	6-Keto-$PGF_{1\alpha}$	$PGF_{2\alpha}$	TxB_2	PGD_2
12					
Sham	1.4 ± 0.4	1.2 ± 0.3	1.3 ± 0.2	0.20 ± 0.03	0.11 ± 0.01
BUO	10.1 ± 1.8*	7.0 ± 4.2*	4.3 ± 0.7*	0.35 ± 0.01*	0.30 ± 0.02*
BUO + SC-560	5.1 ± 1.0†‡	5.4 ± 0.7‡	2.7 ± 0.4†‡	0.29 ± 0.03	0.20 ± 0.02†
24					
Sham	0.95 ± 0.2	2.0 ± 0.2	2.0 ± 2.8	0.74 ± 0.12	0.25 ± 0.04
BUO	5.0 ± 1.2*	4.4 ± 0.7*	4.8 ± 1.3	0.55 ± 0.08	0.43 ± 0.16
BUO + SC-560	4.5 ± 0.6‡	3.2 ± 0.4‡	4.8 ± 1.6	0.59 ± 0.09	0.21 ± 0.03

Values are means ± SE for $n = 6$ rats in each group. Units are pg/μg tissue. $P < 0.05$, respective prostanoids in nontreated BUO vs. sham-operated control rats (*), respective prostanoids in nontreated BUO vs. SC-560-treated BUO rats (†), and respective prostanoids in SC-560-treated BUO vs. sham-operated control rats (‡).

the COX-2 labeling was more widespread, intense, and exclusively associated with the medullary interstitial cells compared with kidneys from sham-operated rats. In sham rats, COX-2 labeling in the kidney medulla was at the limit of detection (Fig. 4, *E* and *G*). There was no visible difference between rats subjected to 2 or 6 h of BUO and sham-operated controls (Fig. 4, *A–D*).

To investigate the time course of the changes in microsomal PGES, semiquantitative immunoblotting experiments were

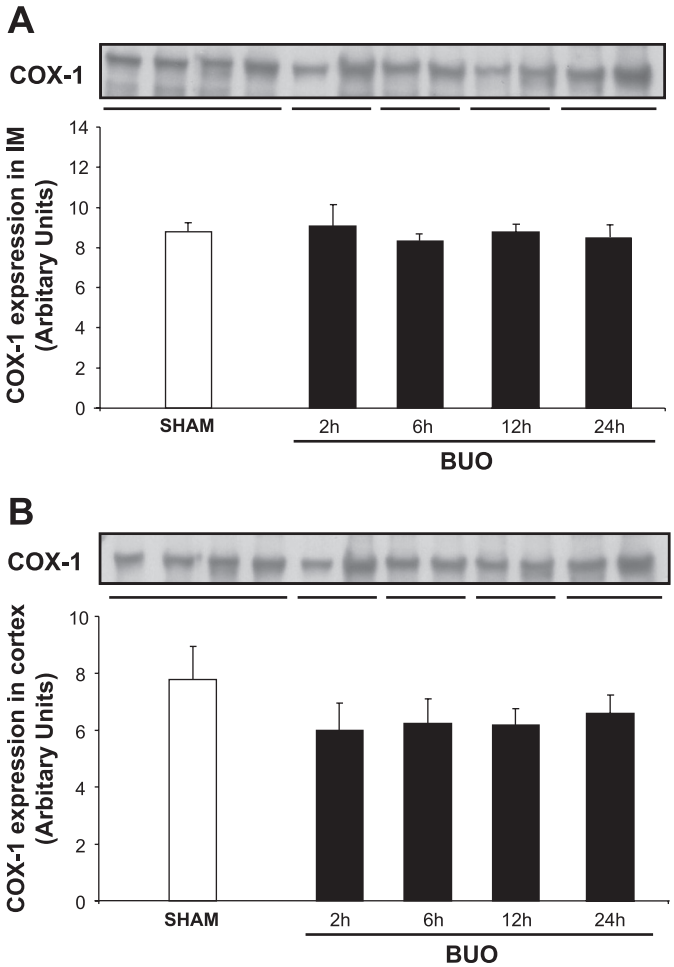

Fig. 2. Semiquantitative immunoblots of cyclooxygenase (COX)-1 using kidney protein isolated from IM and C/OM from bilateral ureteral obstructed (BUO) rats for 2, 6, 12, and 24 h and sham-operated control rats. A total of 20 μg protein was used for the COX-1 assay. *A*: densitometric analysis of all the samples from IM from obstructed kidneys and sham rats revealed that there was no difference between the different time points in the obstructed rats and control. *B*: densitometric analysis of all the samples from C/OM from obstructed kidneys and sham rats revealed that there was no difference between the different time points in the obstructed rats and control.

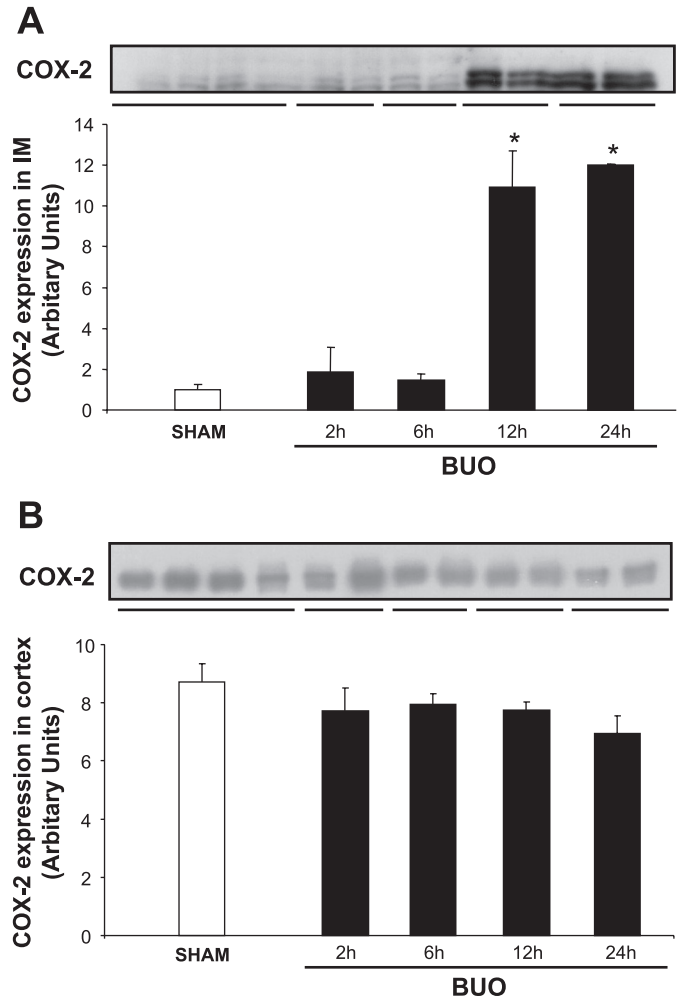

Fig. 3. Semiquantitative immunoblots of COX-2 using kidney protein isolated from IM and C/OM from BUO rats for 2, 6, 12, and 24 h and sham-operated control rats. A total of 30 μg protein was used for the COX-2 assay. *A*: densitometric analysis of all the samples from IM from obstructed kidneys and sham rats revealed that COX-2 protein abundance was increased when rats were subjected to 12 and 24 h BUO compared with control. *$P < 0.05$ vs. control rats in each group. *B*: densitometric analysis of all the samples from C/OM from obstructed kidneys and sham rats revealed that there was no difference between the different time points in the obstructed rats and control.

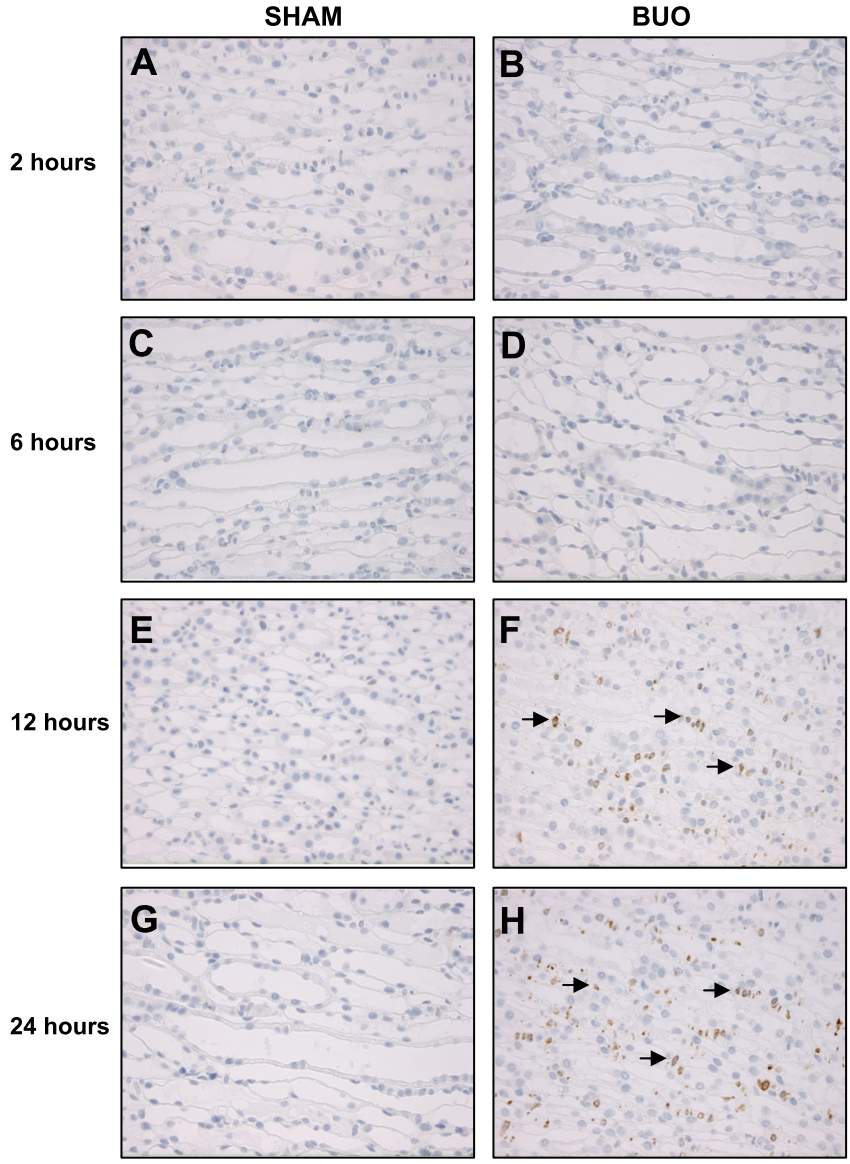

Fig. 4. Immunohistochemistry for COX-2 in kidney IM of sham-operated (*A*, *C*, *E*, and *G*) and BUO rats for 2 (*B*), 6 (*D*), 12 (*F*), and 24 (*H*) h. Only interstitial cells (indicated by arrows) of IM are labeled. There is a strong labeling at the base of IM from obstructed kidneys from 12 (*F*) and 24 (*H*) h, and labeling is not detectable in sham kidneys (*A*, *C*, *E*, and *G*) and obstructed kidneys from 2 (*B*) and 6 (*D*) h.

performed with IM and C/OM. The abundance of PGES protein was unchanged in IM (Fig. 5). There was a tendency toward decreased PGES abundance after 24 h BUO, but this was not significant (Fig. 5*A*). In C/OM, the abundance of PGES protein did not change during the time course of the experiments (Fig. 5*B*).

Effect of the Selective COX-2 Inhibitor on AQP2 Protein Expression in Response to BUO

The time course of the effect of the COX-2 inhibitor parecoxib on AQP2 protein abundance in IM was determined. Semiquantitative immunoblotting for AQP2 was performed with IM protein samples from rats subjected to 2, 6, 12, or 24 h of BUO. The abundance of AQP2 protein in IM was significantly decreased at 12 and 24 h of BUO (Fig. 6). The BUO-induced downregulation of AQP2 was attenuated significantly by administration of the selective COX-2 inhibitor parecoxib at 12 and 24 h (Fig. 6).

DISCUSSION

The main results of the present study were that BUO led to increased tissue concentration of prostanoids (PGE_2, $PGF_{2\alpha}$, TxB_2) predominantly in the renal IM that peaked at 12 h after the occlusion and then largely normalized at 24 h. The prostacyclin metabolite 6-keto-$PGF_{1\alpha}$ peaked after 24 h BUO.

The sum of data support that the acute antidiuretic and natriuretic action of COX-2 inhibitors after release of ureteral obstruction (20) is caused by an action in the renal medulla. Thus, there was a close temporal and spatial correlation between a rise in COX-2 expression in interstitial cells and an increased tissue concentration of prostanoids with arginine vasopressin (AVP)-antagonizing capability in IM, but not in cortex; the IM tissue concentration of PGE_2, PGI_2, $PGF_{2\alpha}$, and TxA_2 all displayed marked sensitivity to a COX-2 inhibitor, and concentrations were essentially normalized or further lowered during BUO, whereas a COX-1 inhibitor had limited

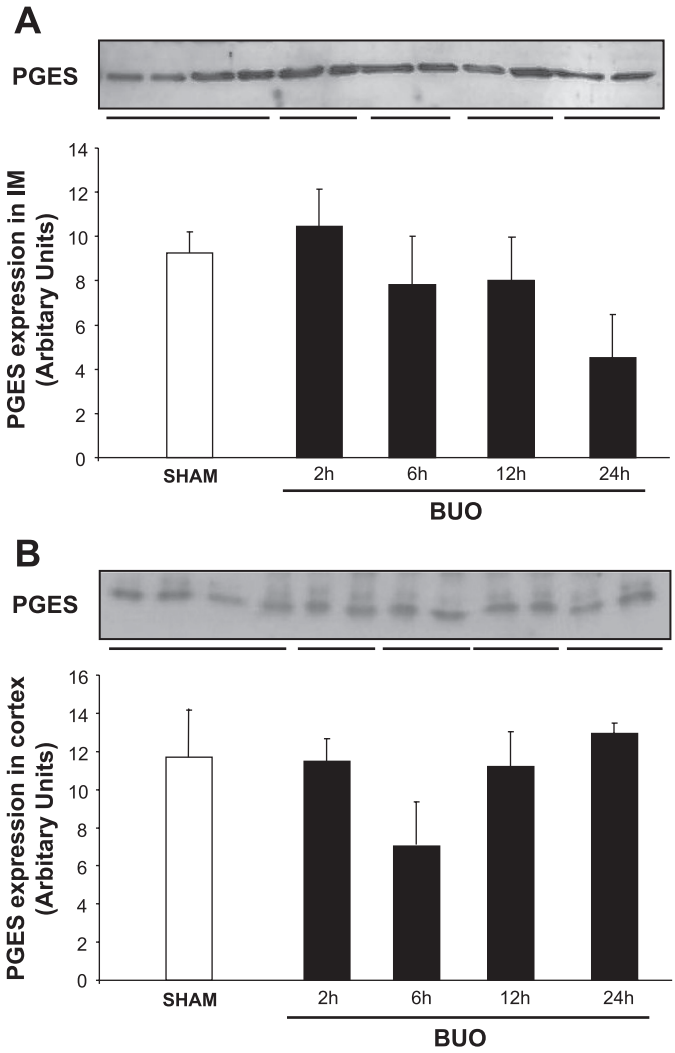

Fig. 5. Semiquantitative immunoblots of PGE_2 synthase (PGES) using kidney protein isolated from IM and C/OM from BUO rats for 2, 6, 12, and 24 h and sham-operated control rats. A total of 30 μg protein was used for the PGES assay. *A*: densitometric analysis of all the samples from IM from obstructed kidneys and sham rats revealed that there was no difference between the different time points in the obstructed rats and control. *B*: densitometric analysis of all the samples from C/OM from obstructed kidneys and sham rats revealed that there was no difference between the different time points in the obstructed rats and control.

effect on PGE_2 and $PGF_{2\alpha}$ concentrations only, and concentrations were not normalized.

The total prostanoid content was one to two orders of magnitude higher in IM than C/OM in rats. This is consistent with previous studies showing an increased total amount of prostanoids in IM compared with cortex in normal rats (11). Moreover, it is in keeping with the expected gradient of the obstruction-mediated impact on kidney tissue where IM is likely to be exposed most rapidly and strongly to increased retrograde pressure gradient and its consequences. The data suggest that COX-2 activity in the inner medullary interstitial cells can provide substrate for an array of downstream prostanoid synthases which indicates either preexisting colocalization or induction of synthases in medullary cells in response to BUO. Indeed, PGES was detected in the IM and has been shown in inner medullary interstitial cells and collecting ducts (25). The PGES can be induced by cytokines and inflammatory stimuli (13), and it is believed that PGES is functionally coupled to COX-2 in the medullary interstitial cells and contributes to PGE_2 biosynthesis in these cells. However, in the collecting ducts, the inducible PGES is coupled to COX-1 (25). Our data support that the collecting duct COX-1-PGES pair contributes to the BUO-induced tissue PGE_2 accumulation. Our data showed that PGES protein expression is not significantly changed in response to obstruction in IM and therefore likely is not a limiting factor. Little data are available with regard to localization of the other prostanoid synthases in kidney tissue. However, studies have shown that prostacyclin synthase mRNA is mainly localized in the vasculature and thromboxane synthase mRNA is detected mainly in glomeruli (28).

In accordance with our observations, it has been demonstrated that BUO for 24 h enhances PGI_2 production in medullary isolated tubules of the rat kidney (29). In contrast with our observations, Yanagisawa et al. (29) also showed increased PGE_2 and TxB_2 levels in medullary isolated tubules in response to 24 h BUO. The literature demonstrates conflicting results regarding the time course of changes of prostanoid tissue concentration in kidney medulla after obstruction. Thus, it was previously demonstrated that PGE_2 and TxB_2 production in papilla and isolated medullary tubules was reduced after 24 h BUO (7). In agreement, the present study showed that PGE_2 and TxB_2 levels returned to control level in IM after 24 h BUO, which indicates that BUO-induced changes in kidney tissue prostanoid concentration are transient, which may reconcile these inconsistent observations. We have not examined the mechanism involved in the transient production of PGE_2, TxB_2, and $PGF_{2\alpha}$ in IM after 24 h BUO.

At one side, prostanoid tissue concentrations were increased at 6 h BUO before measureable changes in COX-2 protein abundance, and, at the other side, COX-2 protein was increased after 24 h BUO, when most prostanoids had returned to control levels. Thus, early activation of phospholipase and liberation of

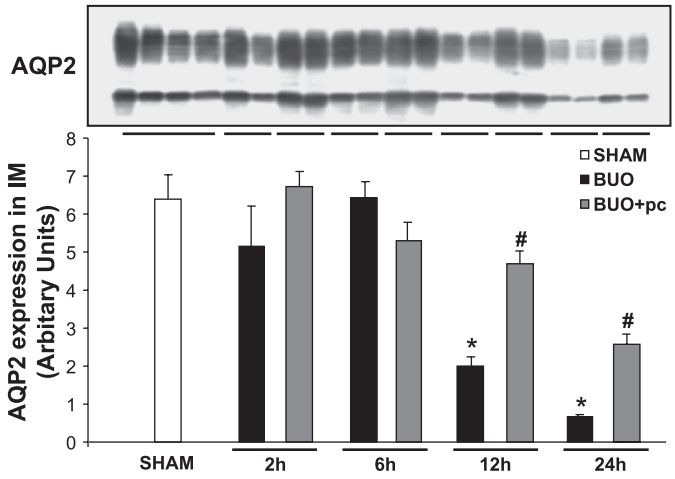

Fig. 6. Semiquantitative immunoblots of aquaporin-2 (AQP2) using kidney protein isolated from IM from nontreated and parecoxib (pc)-treated BUO rats for 2, 6, 12, and 24 h and sham-operated control rats. A total of 10 μg protein was used for the AQP2 assay. Densitometric analysis revealed that AQP2 expression in IM was markedly decreased in rats subjected to BUO for 12 and 24 h compared with sham-operated control rats. Parecoxib treatment of BUO rats prevented this decrease in AQP2 expression. $P < 0.05$ compared with sham-operated rats (*) and with parecoxib-treated BUO rats (#).

arachidonic acid with subsequent metabolization by COX-2, which is present in interstitial cells also in the control situation (1), is probably causing the early increase in tissue prostanoid concentration. This interpretation is supported by the significant effect of the COX-2 inhibitor to lower, e.g., tissue, PGE_2 concentration at 6 h BUO. Beyond 24 h BUO, substrate depletion, lower phospholipase activity, or downstream synthase downregulation could explain normal prostanoid levels despite elevated COX-2 protein levels. Furthermore, prostanoids may exert feedback inhibition (12), and Lemieux et al. (16) demonstrated in renal podocytes that PGE_2 reduces arachidonic acid release in a cAMP/PKA-dependent manner.

In agreement with previous observations in BUO and UUO models, COX-1 expression did not change in response to obstruction in IM (3, 19), but COX-1 activity contributed to BUO-induced accumulation of PGE_2, $PGF_{2\alpha}$, and PGD_2 at 12 h, but prostanoid levels were still significantly elevated, which documents clearly that COX-2 activity is necessary to account for the tissue response to BUO.

The difference in absolute tissue prostanoid concentrations in the COX-1 inhibitor series could have been caused by a longer tissue storage before processing.

Previous studies have indicated that COX-1 predominately contributes to basal prostanoid production in the kidney (11, 22). Although we did not determine the effect of COX blockers in sham-operated animals, our results suggest that both enzymes contribute to tissue levels of renal PGE_2 and $PGF_{2\alpha}$ and that COX-2 preferentially couples to PGI_2 synthesis while, interestingly, renal PGD_2 synthesis appears to be exclusively mediated by COX-1. PGD_2 tissue concentration increased significantly after COX-2 inhibition. This observation could be explained by competition between COX-1 and COX-2 for arachidonic acid in PGD synthase-expressing cells and would be compatible with the observed effect of the COX-1 inhibitor to suppress PGD_2 tissue level.

Ureteral obstruction causes a temporary increase in blood flow during the first 2–5 h in the obstructed kidney, predominantly caused by preglomerular vasodilation, followed by progressive preglomerular vasoconstriction (14). Local production of the vasodilator PGE_2 and PGI_2 was noted after 6 h in C/OM (and IM) and may account for the increased RBF. In accord with data that show a progressive decrease in RBF mediated by ANG II, TxB_2, and endothelin (14), we found an increased production of TxB_2 in C/OM. The increased TxB_2 in IM could contract descending vasa recta and consequently add to the RBF decrease. Imidazole, an inhibitor of thromboxane synthesis, increases medullary blood flow in conscious rats (8). Ureteral obstruction affects tubular function (15). There is a marked diuresis and natriuresis after release of BUO of 24 h duration (9, 20). PGE_2 and PGI_2 not only are vasodilators but also have direct natriuretic and diuretic properties (24). Administration of a selective COX-2 inhibitor to rats subjected to 24 h BUO followed by release of obstruction prevents the increased urinary excretion of PGE_2 and PGI_2 metabolite 6-keto-$PGF_{1\alpha}$; it also lowers diuresis and prevents downregulation of collecting duct AQP2 (20). The present study confirms these observations on AQP2 and supports that enhanced COX-2 expression and activity in the obstructed kidney after 12 and 24 h BUO is involved in the downregulation of AQP2.

Perspectives and Significance

The present study examines the relationship between COX-2/COX-1 expression and tissue prostanoid concentration after acute ureteral obstruction for 2, 6, 12, and 24 h by defining the renal prostanoid profiles in renal tissue using a specific COX-1 and COX-2 inhibitor. Our data indicate that BUO leads to rapid and significant increases in local tissue prostanoid concentration in the renal IM mediated preferentially by increased COX-2 abundance and activity. These findings suggest that local synthesis and accumulation of prostanoids in the renal IM could play a role in the dysregulation of renal tubular function and medullary hemodynamics observed in response to BUO.

ACKNOWLEDGMENTS

We thank Line V. Nielsen, Gitte Kall, Gitte Skou, Inger Merete Paulsen, Dorte Wulff, and Bernhard Watzer for expert technical assistance.

GRANTS

The Water and Salt Research Centre at the University of Aarhus is established and supported by the Danish National Research Foundation (Danmarks Grundforskningsfond). Support for this study was provided by The Karen Elise Jensen Foundation, The Novo Nordisk Foundation, The Commission of the European Union (EU Action Programs), The Danish Medical Research Council, The University of Aarhus Research Foundation, The Danish Cardiovascular Research Academy, The University of Aarhus, and the intramural budget of the National Heart, Lung, and Blood Institute, National Institutes of Health, Katrine and Vigo Skovgaard Foundation, Augustinus Foundation, Beckett Foundation, LEO Pharma Foundation, Grosser L. F. Fogth Foundation, and The A.P. Møller Foundation for the Advancement of Medical Science.

DISCLOSURES

No conflicts of interest are declared by the authors.

REFERENCES

1. **Campean V, Theilig F, Paliege A, Breyer M, Bachmann S.** Key enzymes for renal prostaglandin synthesis: site-specific expression in rodent kidney (rat, mouse). *Am J Physiol Renal Physiol* 285: F19–F32, 2003.
2. **Cheng X, Zhang H, Lee HL, Park JM.** Cyclooxygenase-2 inhibitor preserves medullary aquaporin-2 expression and prevents polyuria after ureteral obstruction. *J Urol* 172: 2387–2390, 2004.
3. **Chou SY, Cai H, Pai D, Mansour M, Huynh P.** Regional expression of cyclooxygenase isoforms in the rat kidney in complete unilateral ureteral obstruction. *J Urol* 170: 1403–1408, 2003.
4. **Dal CA, Corradi A, Stanziale R, Maruccio G, Migone L.** Glomerular hemodynamics before and after release of 24-hour bilateral ureteral obstruction. *Kidney Int* 17: 491–496, 1980.
5. **Frokiaer J, Knudsen L, Nielsen AS, Pedersen EB, Djurhuus JC.** Enhanced intrarenal angiotensin II generation in response to obstruction of the pig ureter. *Am J Physiol Renal Fluid Electrolyte Physiol* 263: F527–F533, 1992.
6. **Frokiaer J, Nielsen AS, Knudsen L, Djurhuus JC, Pedersen EB.** The effect of indomethacin infusion on renal hemodynamics and on the renin-angiotensin system during unilateral ureteral obstruction of the pig. *J Urol* 150: 1557–1563, 1993.
7. **Fukuzaki A, Morrissey J, Klahr S.** Role of glomerular eicosanoid production in the obstructed kidney. *Int Urol Nephrol* 25: 525–531, 1993.
8. **Hably C, Menz V, Bartha J.** Cardiac output distribution and intrarenal haemodynamics: role of thromboxanes. *Acta Physiol Hung* 78: 89–98, 1991.
9. **Harris RH, Yarger WE.** The pathogenesis of post-obstructive diuresis. The role of circulating natriuretic and diuretic factors, including urea. *J Clin Invest* 56: 880–887, 1975.
10. **Hebert RL, Jacobson HR, Breyer MD.** PGE2 inhibits AVP-induced water flow in cortical collecting ducts by protein kinase C activation. *Am J Physiol Renal Fluid Electrolyte Physiol* 259: F318–F325, 1990.

11. **Hetu PO, Riendeau D.** Cyclo-oxygenase-2 contributes to constitutive prostanoid production in rat kidney and brain. *Biochem J* 391: 561–566, 2005.
12. **Hiraishi H, Terano A, Ota S, Ivey KJ, Sugimoto T.** Regulation of prostaglandin production in cultured gastric mucosal cells. *Prostaglandins* 38: 65–78, 1989.
13. **Jakobsson PJ, Thoren S, Morgenstern R, Samuelsson B.** Identification of human prostaglandin E synthase: a microsomal, glutathione-dependent, inducible enzyme, constituting a potential novel drug target. *Proc Natl Acad Sci USA* 96: 7220–7225, 1999.
14. **Klahr S.** Obstructive nephropathy. *Intern Med* 39: 355–361, 2000.
15. **Klahr S, Harris K, Purkerson ML.** Effects of obstruction on renal functions. *Pediatr Nephrol* 2: 34–42, 1988.
16. **Lemieux LI, Rahal SS, Kennedy CR.** PGE2 reduces arachidonic acid release in murine podocytes: evidence for an autocrine feedback loop. *Am J Physiol Cell Physiol* 284: C302–C309, 2003.
17. **Moody TE, Vaughan ED Jr, Gillenwater JY.** Comparison of the renal hemodynamic response to unilateral and bilateral ureteral occlusion. *Invest Urol* 14: 455–459, 1977.
18. **Nielsen J, Kwon TH, Praetorius J, FrokiAEr J, Knepper MA, Nielsen S.** Aldosterone increases urine production and decreases apical AQP2 expression in rats with diabetes insipidus. *Am J Physiol Renal Physiol* 290: F438–F449, 2006.
19. **Norregaard R, Jensen BL, Li C, Wang W, Knepper MA, Nielsen S, FrokiAEr J.** COX-2 inhibition prevents downregulation of key renal water and sodium transport proteins in response to bilateral ureteral obstruction. *Am J Physiol Renal Physiol* 289: F322–F333, 2005.
20. **Norregaard R, Jensen BL, Topcu SO, Diget M, Schweer H, Knepper MA, Nielsen S, FrokiAEr J.** COX-2 activity transiently contributes to increased water and NaCl excretion in the polyuric phase after release of ureteral obstruction. *Am J Physiol Renal Physiol* 292: F1322–F1333, 2007.
21. **Padi SS, Jain NK, Singh S, Kulkarni SK.** Pharmacological profile of parecoxib: a novel, potent injectable selective cyclooxygenase-2 inhibitor. *Eur J Pharmacol* 491: 69–76, 2004.
22. **Qi Z, Cai H, Morrow JD, Breyer MD.** Differentiation of cyclooxygenase 1- and 2-derived prostanoids in mouse kidney and aorta. *Hypertension* 48: 323–328, 2006.
23. **Sakairi Y, Jacobson HR, Noland TD, Breyer MD.** Luminal prostaglandin E receptors regulate salt and water transport in rabbit cortical collecting duct. *Am J Physiol Renal Fluid Electrolyte Physiol* 269: F257–F265, 1995.
24. **Schlondorff D, Ardaillou R.** Prostaglandins and other arachidonic acid metabolites in the kidney. *Kidney Int* 29: 108–119, 1986.
25. **Schneider A, Zhang Y, Zhang M, Lu WJ, Rao R, Fan X, Redha R, Davis L, Breyer RM, Harris R, Guan Y, Breyer MD.** Membrane-associated PGE synthase-1 (mPGES-1) is coexpressed with both COX-1 and COX-2 in the kidney. *Kidney Int* 65: 1205–1213, 2004.
26. **Schweer H, Watzer B, Seyberth HW.** Determination of seven prostanoids in 1 ml of urine by gas chromatography-negative ion chemical ionization triple stage quadrupole mass spectrometry. *J Chromatogr* 652: 221–227, 1994.
27. **Teng XW, bu-Mellal AK, Davies NM.** Formulation dependent pharmacokinetics, bioavailability and renal toxicity of a selective cyclooxygenase-1 inhibitor SC-560 in the rat. *J Pharm Pharm Sci* 6: 205–210, 2003.
28. **Vitzthum H, Abt I, Einhellig S, Kurtz A.** Gene expression of prostanoid forming enzymes along the rat nephron. *Kidney Int* 62: 1570–1581, 2002.
29. **Yanagisawa H, Moridaira K, Nodera M, Wada O.** Ureteral obstruction enhances eicosanoid production in cortical and medullary tubules of rat kidneys. *Kidney Blood Press Res* 20: 398–405, 1997.
30. **Yarger WE, Schocken DD, Harris RH.** Obstructive nephropathy in the rat: possible roles for the renin-angiotensin system, prostaglandins, and thromboxanes in postobstructive renal function. *J Clin Invest* 65: 400–412, 1980.